

## Epitaxial thick films by spray pyrolysis for coated conductors

L. Vergnières<sup>1,2,3</sup>, P. Odier<sup>2</sup>, F. Weiss<sup>1</sup>, C-E. Bruzek<sup>3</sup>, J-M. Saugrain<sup>4</sup>

<sup>1</sup> LMGP-ENSPG-INPG, BP 46, 38402 Saint Martin d'Hères, France.

<sup>2</sup> Laboratoire de Cristallographie-CNRS, BP 166, 38042 Grenoble, France.

<sup>3</sup> Nexans France, 31 rue de l'industrie, 59572 Jeumont, France.

<sup>4</sup> Nexans France, 4-10 rue Mozart, 92587 Clichy, France

### Abstract

Spray pyrolysis has been successfully used to synthesize many oxides, like transparent conducting films ( $\text{SnO}_2$ ,  $\text{ZnO}$  and  $\text{InO}_3$ ) or cuprate-based superconducting films. The technique has a high deposition rate and uses cheap raw materials in non-vacuum environment. In our work spray pyrolysis has been used to grow superconducting epitaxial thick films of  $\text{YBa}_2\text{Cu}_3\text{O}_{7-\delta}$  (YBCO) on textured substrates. A precursor nitrate solution is atomized and carried towards a substrate which is heated between  $800^\circ\text{C}$  and  $900^\circ\text{C}$ . After growth, oxygenation is carried out by cooling under oxygen flow. YBCO films deposited on a single-crystal ( $\text{SrTiO}_3$ ) exhibit a very good c-axis orientation ( $\Delta\omega=0.4^\circ$ ) as well as an in-plane texture ( $\Delta\phi=0.6^\circ$ ). Transport measurement has given  $I_c$  value close to 10A (77K, sf) on a 5 mm wide tape. First YBCO depositions on technical substrates made by ion beam assisted deposition (IBAD) display a quite good out-of-plane texture ( $\Delta\omega=7^\circ$ ) and a  $T_{c_{\text{onset}}}$  of 90K. Furthermore, prospective work on buffer layers ( $\text{Y}_2\text{O}_3$ ,  $\text{CeO}_2$ ,  $\text{CuO}$ ) synthesis has been carried out. Despite the high potential of spray pyrolysis, the mechanisms involved in the deposition are quite unknown. It has been evidenced a narrow relationship between the precursor decomposition and the properties of the deposition. In particular an important difference

between the decomposition temperatures of the precursors implies a modification of the stoichiometry in the film. In certain cases  $\text{NO}_2$  outgassing can be problematic as it can induce cracks or foam morphology.

Keywords: Films (A), Microstructure-final (B), Oxide superconductors (D), Spray pyrolysis

## I. Introduction

In the past few years, intensive efforts have been orientated towards the preparation of long flexible HTS tapes mainly for transformers, magnets, transmission cables, generators and fault current limiter applications. Coated conductor technology, based on the deposition of YBCO films on long flexible substrates, has produced conductors with  $J_c > 1 \text{ MA/cm}^2$ . But it has not yet been established which technique is the most appropriate for industrial applications and it is of a great importance to extend the investigations. In this paper we focus on ultrasonic spray pyrolysis. The technique has the great advantage of combining high deposition rates in a non-vacuum environment and low cost raw materials (nitrates). Results on buffer layers deposited by spray pyrolysis are first reported then the performances of YBCO films on single-crystal and IBAD substrates are presented.

## II. Experimental

Y, Ba and Cu nitrate solutions were made by dissolving separately  $\text{Y}_2\text{O}_3$ ,  $\text{BaCO}_3$  and  $\text{CuO}$  in an aqueous solution of nitric acid. The final precursor solution was made by mixing the individual solutions with the appropriate cation ratio. The concentration of the overall solution is 0.3 mol/L. The solution of cerium nitrate was obtained by dissolving  $\text{Ce}(\text{NO}_3)_3$  in deionised water. The nitrate solution was sprayed into a mist using an ultrasonic generator that produces droplets of 15-20  $\mu\text{m}$  in size. The mist was carried by argon onto the substrate

which was heated around 850°C. The spray was generated for 10 min. After growth, oxygenation was carried out by a controlled cooling to room temperature under oxygen flow. The films were characterized by SEM, X-ray diffraction,  $\chi_{ac}$  susceptibility and transport  $I_c$ .

### III. Results and discussions

#### III.1 Buffer layers

##### III.1.1 $Y_2O_3$ and $CeO_2$

Prospective work on the synthesis of buffer layers by nitrate spray pyrolysis has been started. First  $Y_2O_3$  and  $CeO_2$  depositions have been performed at 700°C under a flow of argon. In both cases we did not obtain continuous and dense films but sparse foams, made of hollow and cracked spheres. To determine the cause of this morphology we have investigated the decomposition of nitrate powder. In a previous work [1] we had shown that yttrium nitrate powder placed in a crucible and heated up to 850°C in a furnace under an argon flow led to  $Y_2O_3$  foam because of a  $NO_2$  outgassing in a very viscous liquid. The important result is to stress that the morphology of the film depends, at least partly, on the mechanisms of nitrate decomposition. The morphology could probably be improved by a desegregation of the foams before deposition, by an increase in temperature or in nozzle-substrate distance.

##### III.1.2 $CuO$

$CuO$  films have been obtained at 400°C under argon flow. Fig.1 shows a X-ray diffraction patterns ( $\theta/2\theta$ ) of a  $CuO$  film. The film exhibits a (111) texture and a smooth surface. The decomposition of copper nitrate powder leads to the formation of a fine powder of  $CuO$  above 300°C. Such morphology is favourable to an epitaxial film formation. Textured  $CuO$  films might be useful as a seed layer to grow epitaxial films of YBCO.

## III.2 YBCO films on single-crystal

### III.2.1 Composition

The composition of the precursor solution is not conserved in spray pyrolysis. For this reason the first step to process is an adjustment of the stoichiometry in the starting solution. We have found the optimal value of the cationic ratio to be Y:Ba:Cu=1:2:1. It is interesting to note that most authors use a stoichiometry close to 1:2:x [2-4]. Therefore the ratio Y:Ba is independent from experimental conditions and moreover it is equal to the initial ratio. Copper is deposited at a higher rate. We can explain the preferential deposition of copper by the fact that copper nitrate is already decomposed in oxide when it hits the substrate ( $T_{\text{CuO formation}} \approx 300^\circ\text{C}$ ) while barium and yttrium are pushed back from the substrate by  $\text{NO}_2$  outgassing which occurs during precursors decomposition on the substrate ( $T_{\text{Y}_2\text{O}_3 \text{ formation}} \approx 550^\circ\text{C}$  et  $T_{\text{BaO formation}} \approx 700^\circ\text{C}$ ).

### III.2.2 Microstructure

The films microstructures vary drastically in a narrow temperature range and have important effects on the superconducting properties. Three different microstructures M1, M2 and M3 have been obtained for films deposited on substrates, which have been heated respectively at 840, 850 and 860°C. The microstructural and superconducting properties (grains size,  $\phi$ -scan,  $\omega$ -scan, proportion c-axis/ab-plan growth,  $T_c$ ) are reported in the Tab.1. Fig.2 shows SEM photographs of the films cross sections. First statement is that grains size increases strongly with temperature: it is  $<1 \mu\text{m}$  for a deposition temperature of 840°C and  $>10 \mu\text{m}$  at 860°C. Moreover the proportion of c-axis growth compared with ab-plan growth is larger at 860°C (92%) than at 840°C (66%). We note that  $\phi$ -scan and  $\omega$ -scan FWHM values are not significantly changed. Nevertheless no  $\chi$  ac transition has been detected for M3, and M1 exhibits a broad transition at low temperature. Only M2 displays a narrow transition at 90K.

At 840°C some porosities are observed (Fig.4) inside the film, which are caused by the crossing of c-axis and ab-plan grains. Moreover the diffusion of the cations is not very active as shown by the small grains size and impurities are probably trapped in the film. These defects generate a broad  $\chi_{ac}$  superconducting transition. At 860°C a larger diffusion enables the growth of large grains and an efficient mixture of the species. But a XRD peak at  $2\theta=36.6^\circ$  reveals the presence of a non-identified phase, which is probably a reaction phase with the substrate, that precludes the  $\chi_{ac}$  superconducting transition. Therefore the best microstructure is a compromise between a maximum of c-axis growth and an absence of parasite phase. It was found for a temperature of  $850^\circ\text{C} \pm 3^\circ\text{C}$ .

### III.2.3 Superconducting properties

The best YBCO films deposited on  $\text{SrTiO}_3$  single-crystals display a  $T_c=90\text{K}$  with  $\Delta T=1\text{K}$ .  $J_c$  measured by a.c. susceptibility are regularly larger than  $1 \text{ MA/cm}^2$  (77K, sf) for a thickness of  $1 \mu\text{m}$ , showing a good homogeneity of the film volume. Fig.3 shows transport measurement on a 5 mm wide tape.  $I_c$  value is close to 10A (77K, sf).

### III.3 YBCO films on IBAD substrate

YBCO films have been deposited on YSZ-IBAD substrates covered with a homo-epitaxial YSZ layer deposited by MOCVD [5]. Fig.4 displays the  $\theta/2\theta$  scan of this film: YBCO-film is c-axis textured as revealed from the enhanced  $00\ell$  peaks. The out-of-plane texture (005) is rather good ( $\text{FWHM}=7^\circ$ ) but the in-plane texture (103) ( $\text{FWHM}>35^\circ$ ) needs to be improved. Perhaps the rather large mismatch of YBCO with YSZ ( $\sim 6\%$ ) accounts for the absence of in-plane texture. Fig. 5 shows a  $\chi_{ac}$  transition of such an YBCO film with a  $T_c$  onset of 90K and a  $T_c$  endpoint of 75K. The broad transition is probably due to the presence of impurities and porosities in the film.

## Conclusion

Nitrate Spray pyrolysis is an efficient method for YBCO films synthesis. A suitable microstructure requires the absence of ab-plan growth and parasite phases, and has been obtained around 850°C in a temperature range of 5°C. It has been not yet elucidated if the critical evolution of the microstructure versus temperature is caused by kinetic or thermodynamic factors. The synthesis of simple oxides (as buffer layers) strongly depends on the characteristics of the precursors. Y<sub>2</sub>O<sub>3</sub> and CeO<sub>2</sub> morphologies are disadvantaged by foams formation, while CuO fine powders make possible the growth of an epitaxial film.

## Acknowledgments

The authors would like to thank the Association Nationale de la Recherche Technique (ANRT) and Nexans for financial support. Anca Antonevici and Daniel Bourgault are thanked for I<sub>c</sub> transport measurements. The author expresses his gratitude to Sébastien Donet and Carmen Jimenez for the YSZ buffer and Ag cap layers deposition by MOCVD.

## References

- [1] Vergnières, L., Precursors physico-chemical properties and influence on the morphology and stoichiometry of films deposited by spray pyrolysis for YBCO synthesis, EUCAS 2003, in press.
- [2] MacManus-Driscoll, J.L., In-plane aligned YBCO thick films grown in situ by high temperature ultrasonic spray pyrolysis, Superconductor Science and Technology, 2001, **14**, pp. 96-102.
- [3] Shields, T.C., Deposition of YBCO films by high temperature spray pyrolysis, Physica C, 2002, **372-376**, pp. 747-750.

[4] Liu, M., A newly designed ultrasonic spray pyrolysis device to fabricate YBCO tapes, *Physica C*, 2003, **386**, pp. 366-369.

[5] Donet, S., Reel to reel MOCVD for YBCO coated conductor, *IEEE-Transactions-on-applied-superconductivity*, 2003, **13(2)**, pp.2524-7.

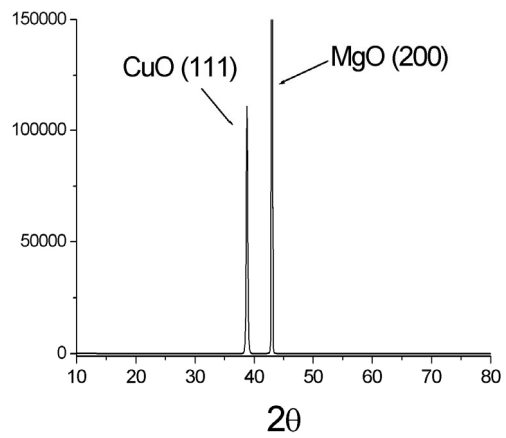


Fig.1 XRD pattern ( $\theta/2\theta$ ) of a CuO film deposited on a MgO single-crystal.



	M1	M2	M3
Grain size	<1 $\mu\text{m}$	$\sim 1\text{-}2 \mu\text{m}$	>10 $\mu\text{m}$
Texture (103) (005)	$\Delta\phi=1.0^\circ$ $\Delta\omega=0.6^\circ$	$\Delta\phi=0.6^\circ$ $\Delta\omega=0.6^\circ$	$\Delta\phi=0.6^\circ$ $\Delta\omega=0.8^\circ$
c-axis growth proportion	66%	75%	92%
Tc (a.c. susceptibility)	Tc=82K $\Delta Tc=3K$	Tc=90K $\Delta Tc=1K$	No screening

Tab.1 Microstructures (grains size, in-plane and out-of-plane textures, c-axis/ab-plan growth proportion, Tc) of YBCO films deposited respectively at 840, 850 and 860°C on SrTiO<sub>3</sub> single-crystals.

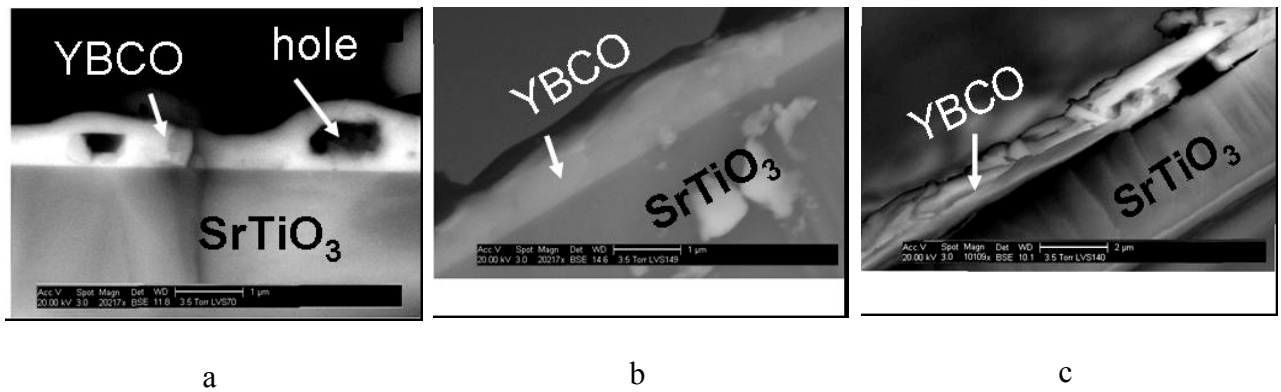


Fig. 2 SEM photographs of cross sections of YBCO films deposited on SrTiO<sub>3</sub> single-crystals. The corresponding microstructural characterizations are reported in the tab 1. a)M1  
b) M2 c)M3

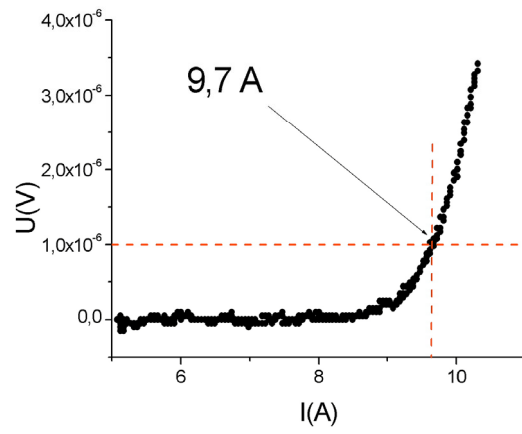


Fig.3.  $I_c$  (77K, sf) transport measurement of a 5 mm wide YBCO film deposited on a  $\text{SrTiO}_3$  single crystal.

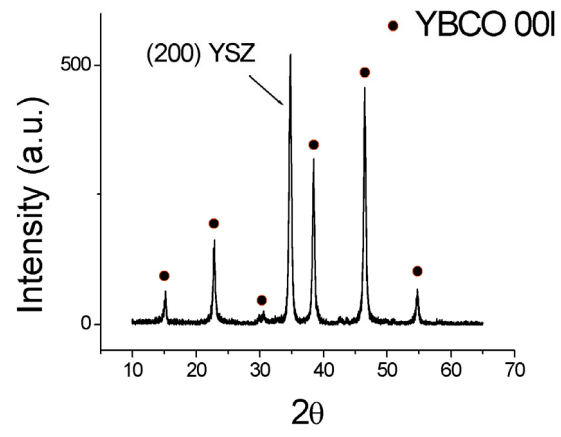


Fig.4 XRD pattern ( $\theta/2\theta$ ) of a YBCO film deposited on a YSZ-IBAD substrate.

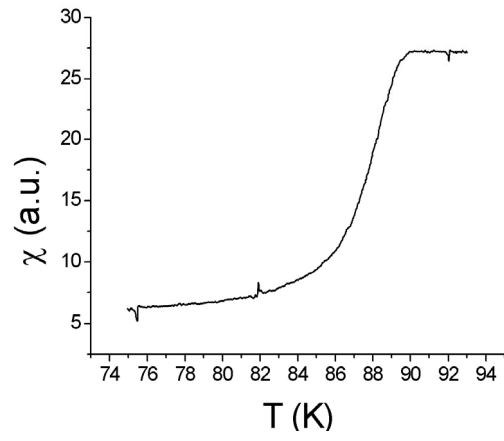


Fig.5  $\chi$  ac measurement of an YBCO film deposited on a YSZ-IBAD substrate.